RADIOCARBON MASS BALANCE FOR A MAGNOX NUCLEAR POWER STATION

M.P. METCALFE, R.W. MILLS

National Nuclear Laboratory, Reactor Operations Support, United Kingdom

Abstract

Nuclear power generation in the United Kingdom is based principally on graphite-moderated gas-cooled reactors. The mass of irradiated graphite associated with these reactors, including material from associated experimental, prototype and production reactors, exceeds 96,000 tonnes. One of the principal long-lived radionuclides produced during graphite irradiation is radiocarbon (C-14), which has a half-life of 5730 ± 40 years. Decommissioning and graphite waste management strategies must take account of this radionuclide. In order to identify appropriate options for addressing the potential hazard of C-14, it is important that the production processes are understood and the distributions and concentrations of C-14 are characterised.

In fact, C-14 precursors and their activation processes are well-known. However, there is ongoing debate over the relative importance of different C-14 precursors, which will determine the location of C-14 within graphite components and hence its mobility/response to treatment. A generally held misconception concerning C-14 in irradiated graphite is that generic statements can be made about its precursors and their location. C-14 location and activities will depend upon the composition of the original manufactured graphite (raw materials, impurities), the chemical environment of the graphite during service and the irradiation history of the graphite. So, while there may be some similarities across, for example, carbon dioxide cooled graphite moderated designs (Magnox, AGR, UNGG), any informed assessment of a core's C-14 inventory would require more-precise characterisation.

The analysis presented here focuses on a UK Magnox reactor core, Reactor 1 at Wylfa Nuclear Power Station. The objective of the analysis is to present a full C-14 mass balance over a selected period of operation for which there are accurate C-14 discharge records. The analysis presented here provides the first assessment of the principal C-14 activation pathways for a UK Magnox reactor . Activation modelling is used to predict C-14 production rates in both the graphite core and the carbon dioxide coolant. Predictions for the graphite are benchmarked against C-14 analyses undertaken on samples taken from the Wylfa cores. Given the uncertainties in the analysis, a precise mass balance between C-14 production and C-14 discharged to the atmosphere is not expected. However, the analysis is shown to be capable of identifying principal activation routes, which should inform future graphite waste management strategies relating to radiocarbon.

1. INTRODUCTION

Nuclear power generation in the United Kingdom is based principally on graphite-moderated gas-cooled reactors. The mass of irradiated graphite associated with these reactors, including material from associated experimental, prototype and production reactors, exceeds 96,000 tonnes [1]. One of the principal long-lived radionuclides produced during graphite irradiation is radiocarbon (C-14), which has a half-life of 5730 ± 40 years (JEF-2.2). Decommissioning and graphite waste management strategies must take account of this radionuclide. In order to identify appropriate options for addressing the potential hazard of C-14, it is important that the production processes are understood and the distributions and concentrations of C-14 are characterised.

In fact, C-14 precursors and their activation processes are well-known (see for example [2,3]). However, there is ongoing debate over the relative importance of different C-14 precursors, which will determine the location of C-14 within graphite components and hence its mobility/response to treatment. A generally held misconception concerning C-14 in irradiated graphite is that generic statements can be made about its precursors and their location. C-14 location and activities will depend upon the composition of the original manufactured graphite (raw materials, impurities),

graphite mass loss due to radiolytic oxidation, the chemical environment of the graphite during service and the irradiation history of the graphite. So, while there may be some similarities across, for example, carbon dioxide (CO_2) cooled graphite moderated designs (Magnox, Advanced Gas-Cooled (AGR), Uranium Naturel Graphite Gaz (UNGG)), any informed assessment of the C-14 inventory of a core would require more-precise characterisation.

The analysis presented here focuses on a UK Magnox reactor core, Reactor 1 at Wylfa Nuclear Power Station. The objective of the analysis is to present a full C-14 mass balance over a selected period of operation for which there are accurate C-14 discharge records. The analysis presented here provides the first assessment of the principal C-14 activation pathways for a UK Magnox reactor. Activation modelling is used to predict C-14 production rates in both the graphite core and the CO_2 coolant. Predictions for the graphite are benchmarked against C-14 analyses undertaken on samples taken from the Wylfa cores. Given the uncertainties in the analysis, a precise mass balance between C-14 production and C-14 discharged to the atmosphere may not be possible. However, the analysis should be capable of identifying principal activation routes, which should inform future graphite waste management strategies relating to radiocarbon.

1.1. Formation of C-14

C-14 is a radioactive isotope of carbon. It is produced in the atmosphere by the capture of thermal neutrons produced from cosmic rays by nitrogen atoms (specifically N-14). C-14 can also be produced through thermal neutron capture on naturally occurring isotopes of carbon (C-13) and oxygen (O-17):

$$N\text{-}14 + n \longrightarrow C\text{-}14 + p$$

$$C\text{-}13 + n \longrightarrow C\text{-}14 + \gamma$$

$$O\text{-}17 + n \longrightarrow C\text{-}14 + \alpha$$

In the case of radiocarbon produced in the atmosphere, this makes no contribution to C-14 levels in as-manufactured Magnox reactor graphite (PGA graphite) as this graphite is manufactured from fossil fuel products in which C-14 is fixed and will have decayed. C-14 in irradiated graphite will therefore come from N-14, C-13 and O-17 impurities in the material, noting the neutron capture cross-sections and isotopic abundances summarised below:

TABLE 1. THERMAL NEUTRON "2200 m/s" CROSS-SECTIONS PRODUCING C-14 AND ISOTOPIC ABUNDANCES OF THE PRECURSORS [4]

Species	Capture Cross-Section leading to C-14 (Barns)	Isotopic Abundance (%)
N-14	1.86 ± 0.03	99.63 (N-14:Nitrogen)
C-13	0.00137 ± 0.00004	1.11 (C-13:Carbon)
O-17	0.235 ± 0.010	0.037 (O-17:Oxygen)

1.2. Monitoring C-14 discharges at licensed nuclear sites

The Environment Agency sets limits and levels on the discharges of gaseous and liquid radioactive waste from nuclear licensed sites in England and Wales [5]. These are based upon statutory guidance from the UK government, requiring operators to use "best available techniques" (BAT) to minimise the generation and disposal of radioactive waste such that the resulting radiological impact to the

public is brought down to levels that are as low as reasonably achievable. Limits are set for a rolling 12-month period, based on discharges determined on a monthly basis.

In the case of the Wylfa nuclear site, records of daily C-14 discharges (GBq) are maintained for each reactor. These are based upon C-14 activities (Bq m^{-3}) measured in the discharge route, which can be assigned to CO_2 releases from the pressure circuits via controlled "blowdowns" (to control reactor pressure) and from normal losses from the coolant circuits during operation.

For the purposes of this study, the period of operation between consecutive statutory outages on Reactor 1 commencing in September 2009 and ending in August 2011 has been selected. The C-14 discharge data together with the reactor thermal power for this period are summarised in Fig. 1. The data show a sharp rise in C-14 discharges as the reactor comes up to full power, after which discharges level off. The significant rise in the discharge in the final month corresponds to the depressurisation of the coolant circuits and the release of approximately 235 t of CO_2. It should be noted that following such an event, the reactor gas circuits are put through a series of CO_2 pressure/depressurisation cycles to purge the system of air prior to power generation. It is the data from Figure 1 that will be used in the C-14 mass balance analysis detailed below.

For the mass balance presented here, activation modelling will be applied both to the graphite and to the carbon dioxide coolant gas and consideration will be given to the contributions to the C-14 inventory from each of these activation pathways.

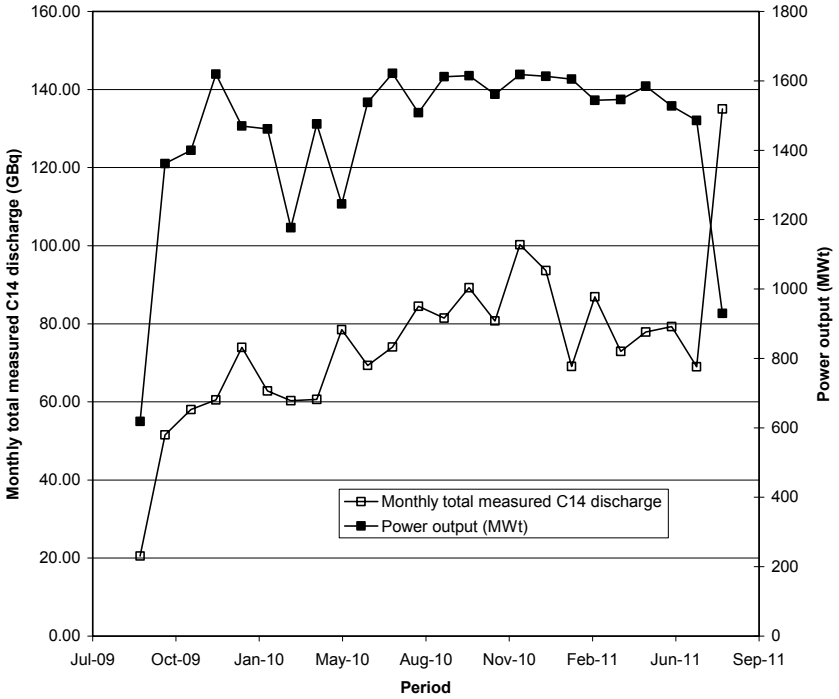

FIG. 1. Summary of C-14 monthly discharge data and associated reactor thermal power – Wylfa Reactor 1.

1.3. Previous related studies

An attempt to rationalise C-14 production in Magnox reactor cores with measurements in gaseous effluents has been reported in [6], where it was concluded that accurate C-14 predictions were impossible because of large uncertainties in impurity levels. Measurements taken at four Magnox sites were reported, together with predictions specifically for Wylfa. Analysis of gaseous effluents provided C-14 activities (in MBq t^{-1} CO_2). Predicted C-14 concentrations in the coolant gas were reported, but the precise method employed was not described. The authors describe source terms as C-13 and N-14 in the moderator, carbon and oxygen in the CO_2 coolant and nitrogen impurity in the

CO_2 coolant (50 volume parts per million). It was noted that predictions were critically dependent upon nitrogen impurity levels and that a level of 7 weight parts per million (wppm) in the graphite would give a C-14 concentration in the coolant equivalent to that from C-13. . The precise method for estimating this value is not explained, but appears to be a simple equating of reaction rates based upon estimates of thermal cross-sections, natural abundance and atomic weights. Using current data and uncertainties from Table 1 above, a nitrogen value of 8.8 ± 0.3 wppm can be calculated, assuming other C-14 producing nuclides (e.g. O-17) are not present. Such estimations do not take account of the full energy spectra of neutrons in the graphite of a Magnox reactor that vary both with location due to neutron transport and time due to graphite loss by oxidation and fuel burn-up effects that are discussed further below.

Bush and co-workers have reported a C-14 waste management study [7] covering a large range of reactor systems including Magnox. Fluxes in various regions of an illustrative Magnox reactor core were used in conjunction with 2200 m s^{-1} cross sections and Westcott's method for adjusting cross-sections with temperature to perform activation calculations. Core parameters and impurity levels were selected on the basis of contemporary UK experience. The study concluded that C-14 arisings were dominated by the graphite moderator and specifically those from C-13 and N-14. The nitrogen impurity level was taken to be 10 wppm. At this level, their calculations showed that N-14 activation accounted for 61% of the total C-14 production. Bush and co-workers also noted that nitrogen depletion by neutron reaction was not expected over a 30-year operating life, broadly consistent with the low N-14 depletion of a few percent seen in calculations in this work. C-14 production in the coolant gas was also evaluated.

2. ASSESSMENT METHODOLOGY

2.1. Mass balance model

For simplicity, the reactor has been divided into two systems: the graphite core and the coolant gas circuits. The graphite core model provides an input term for the coolant gas circuits model and predictions can be benchmarked against actual C-14 measurements on Wylfa core graphite. The coolant gas circuits model, with the output from the graphite core model, provides the total amount of C-14 in the gaseous phase which can be compared with the recorded station discharge data presented in section 1.2. The graphite core model is illustrated schematically in Fig. 2. The boxes on the left hand side of the figure are inputs to the C-14 inventory of the graphite core. The boxes on the right hand side are outputs, being C-14 pathways from the graphite core to the coolant gas circuits.

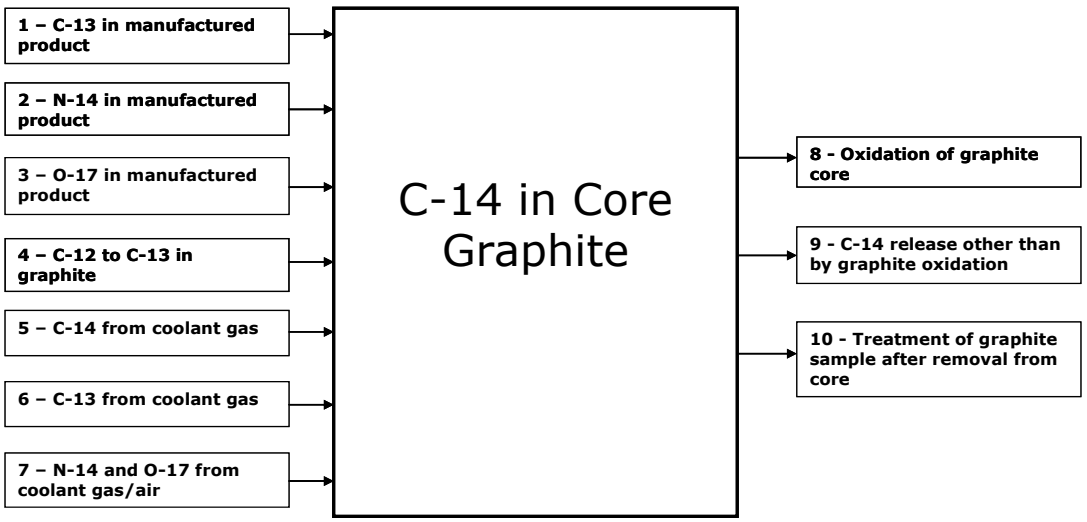

FIG. 2. Schematic representation of graphite core model showing C-14 inputs and outputs.

Taking the graphite core model inputs from top left, boxes 1-3 represent C-14 precursors that may be present as impurities in the manufactured graphite. Box 4 represents the activation of C-12 to C-13, which in turn can be activated to C-14. Boxes 5 and 6 represent additional gas phase contributions to the C-14 inventory either directly (as C-14) or indirectly (via C-13) in the form of carbonaceous deposits that are known to be produced in CO_2 environments. The final input box 7 represents an additional source of N-14 present both as an impurity in the CO_2 coolant and from air when the reactor is depressurised during a statutory outage. In this case, the nitrogen may become physically or chemically attached to the surface of the graphite and be activated to C-14. For outputs from the same model, box 8 represents gasification of the core graphite by radiolytic oxidation with the co-release of C-14. Calculations show the release from the graphite of the radiocarbon precursor C-13 by this mechanism will be insignificant. Box 9 is a catch-all for other release mechanisms that might include, for example, thermal diffusion of C-14 to surfaces and/or thermal release mechanisms. The final output box 10 has been included for completeness as the C-14 inventory of a piece of core graphite may change after removal from the core through treatment (heating, oxidation, machining).

The coolant gas circuits model is illustrated schematically in Fig.3. The boxes on the left hand side of the figure are inputs to the C-14 inventory of the coolant gas. The boxes on the right hand side are outputs, being C-14 pathways to the reactor discharge system and the environment.

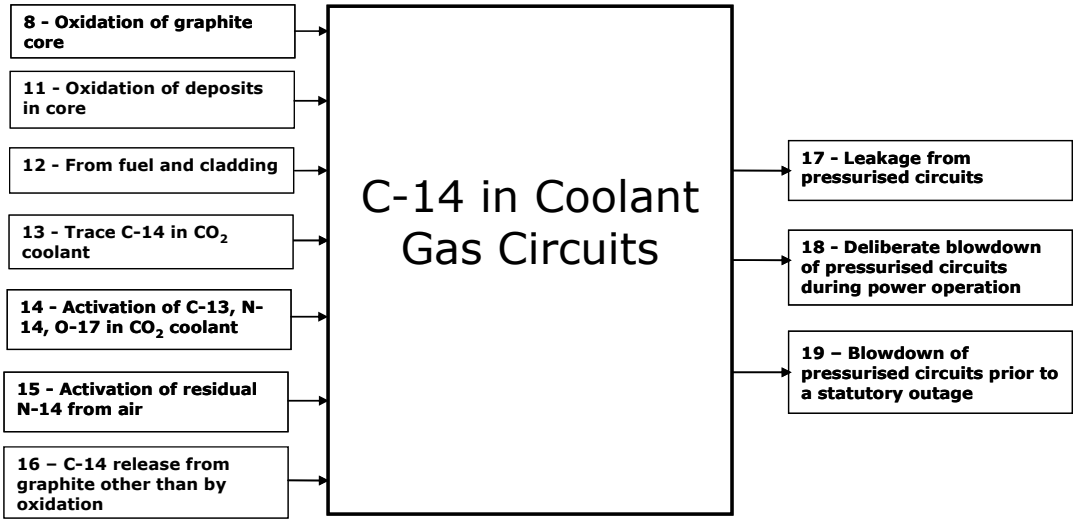

FIG. 3. Schematic representation of coolant gas circuits model showing C-14 inputs and outputs.

Taking the coolant gas circuits model inputs from top left, boxes 8 and 11 represent release of C-14 via radiolytic oxidation of carbonaceous deposits and the underlying graphite. The fuel and cladding in Magnox reactors (box 12) can contain significant levels of C-14 [8] and this could be an input if there were a mechanism for release. Boxes 13 and 14 provide C-14 pathways via the gas coolant itself: some of the carbon making up the CO_2 may be C-14; the coolant gas may contain C-14 precursors (C-13, N-14, O-17) which could become activated. Box 15 covers the possibility that there may be nitrogen from air still present in the gas circuits after a statutory outage that could become activated. The final input box 16 covers C-14 release mechanisms from the graphite core other than oxidation (for example, thermal processes). The three output boxes 17-19 represent release of C-14 with CO_2 gas from continuous leakage from the gas circuits, from deliberate blowdown activities at power and from blowdown of pressurised circuits prior to a statutory outage.

For the purposes of the current analysis, an abbreviated model has been employed and the rationale for such an approach is explained in the following section.

2.2. Abbreviated mass balance model for current analysis

The mass balance model described in section 2.1 attempts to include all C-14 pathways and provides future users with a framework for a more comprehensive assessment. For the current analysis, an abbreviated model has been used and the reasons for omitting selected pathways are explained. The outcome of the C-14 mass balance will provide some indication of how significant the omission of inputs has been. Fig. 4 shows the abbreviated graphite core model with the pathways selected for assessment shown in grey.

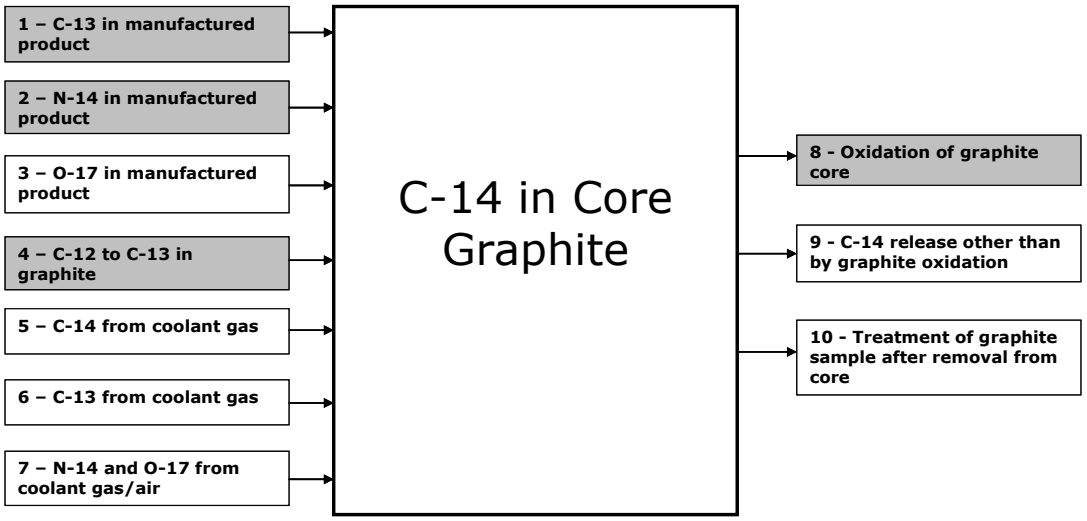

FIG. 4. Schematic representation of abbreviated graphite core model showing C-14 inputs and outputs highlighted in grey.

The contribution from O-17 in the manufactured product (box 3) has been omitted because impurity levels are not known, but are probably insignificant; the isotopic abundance is very low and the thermal neutron capture cross-section is relatively low (see Table 1).

The other three omitted inputs (boxes 5-7) rely upon mechanisms which would bind (either physically or chemically) C-14 or C-14 precursors (C-13, N-14 and O-17) present in the coolant gas or air to the surfaces of the graphite. While their contributions to the C-14 inventory of the graphite may be of interest when assessing the potential activity of graphite core components, there is insufficient information on these pathways to enable quantification. In the context of a C-14 mass balance, contributions to the C-14 inventory of the graphite/gas coolant circuit system from those impurities in the CO_2 gas coolant (as opposed to those from exposure of the core to air) would in any case be accounted for by activation modelling of the gas coolant. There is substantial experimental evidence for carbonaceous deposits being formed on graphite surfaces during operation (see for example [9]). As with the impurities in the CO_2 gas coolant, their activities would be accounted for by activation modelling of the gas coolant. In the case of N-14 in the coolant gas or in air (box 7), it can be adsorbed on graphite surfaces, as illustrated by Brunauer–Emmett–Teller (BET) methods for measuring surface area of activated carbons using nitrogen [10]. There is also evidence for adsorbed nitrogen chemically binding to graphite surfaces under irradiation [11]. However, the significance of such processes on the C-14 inventory of the graphite core of a Magnox reactor is judged to be low due to the low concentrations of nitrogen (in the coolant gas), low binding efficiencies and likely removal by radiolytic oxidation if activated to C-14.

Two outputs have been omitted: box 9 was simply included in the model as a reminder that release mechanisms other than that by radiolytic oxidation may be reducing the C-14 inventory of the graphite (but none have been identified), box 10 covering treatment is not relevant to the current assessment.

Fig. 5 shows the abbreviated gas coolant circuits model with the pathways that will be assessed shown in grey.

Release of C-14 to the coolant from oxidation of C-14-containing carbonaceous deposits (box 11) is not relevant to a mass balance as these deposits are formed from the coolant and its impurities and their contribution should already have been accounted for in coolant activation calculations.

It is recognised that the fuel and cladding of Magnox reactors may contain significant levels of C-14 (boxes 11 and 12). While this may be an issue for the disposal of these materials during decommissioning, there is no mechanism for the release of C-14 during normal reactor operation and therefore no contribution to the mass balance.

While there is the potential for C-14 to be present within the carbon forming the CO_2 coolant (box 13), gas supplied to the Magnox stations is a by-product of the fertilizer industry from mineral sources and consequently any C-14 will be fixed and have decayed.

Activation of residual N-14 from air (box 15) is difficult to quantify but the sensitivity of the mass balance to any contribution via this pathway can be addressed by varying the impurity levels in the CO_2 (addressed below). C-14 release from the graphite by mechanisms other than oxidation (box 16) has been discussed above in the context of the abbreviated graphite core model: no such mechanisms have been identified.

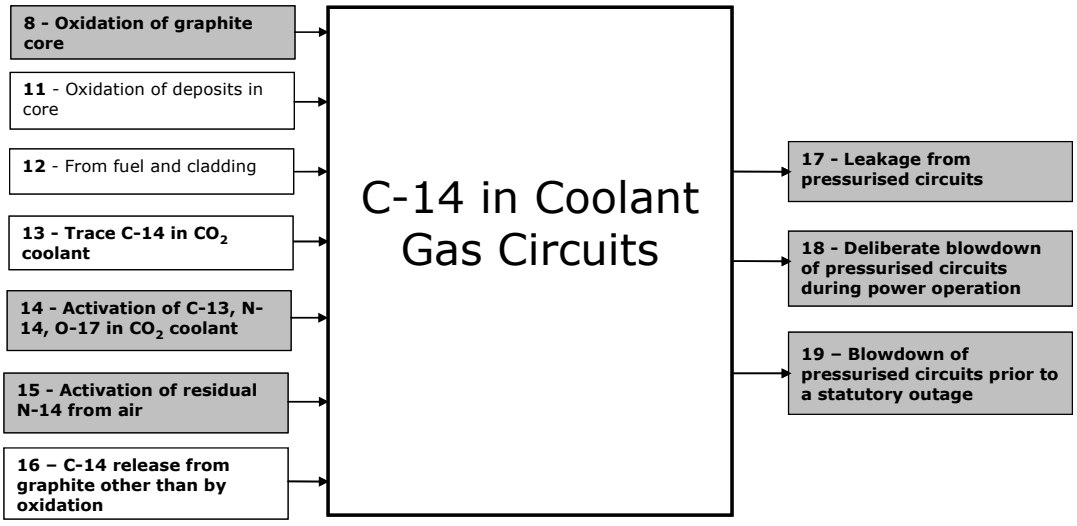

FIG. 5. Schematic representation of abbreviated gas coolant circuits model showing C-14 inputs and outputs highlighted in grey.

3. MASS BALANCE

3.1. Prediction of C-14 production in core graphite by activation modelling

C-14 production in core graphite has been estimated using activation modelling, based upon the reactor physics code MCNPX [12] and the fuel inventory code FISPIN [13]. By specifying concentrations of C-14 precursors in the graphite (natural abundance of C-13 and an assumed concentration of N-14) and with the code allowing for the activation of C-12 to C-13 to C-14, C-14 productions rates can be calculated. The most practical method of demonstrating the accuracy of activation calculations is to benchmark calculations against experimental measurements. In this case, a model was set up specifically for the Wylfa Reactor 1 core, with predictions targeting a position in the core where such measurements had been made [14].

The MCNP model consisted of a parallelepiped of graphite vertically through the complete height of the reactor with reflective boundary conditions, except for the top and bottom, which were modelled as non-reflective boundaries. The model included the minimum unique repeating cell that represented the core, which within the modelled graphite block model comprised four fuel channels, a control rod channel and an interstitial channel containing the sample holder and samples (prepared from the same graphite used to construct the core) that provided the experimental measurements. For the modelling of the samples, the fuel was modelled as a continuous uranium metal rod and cladding with a length equal to the active height of the reactor reactor with the irradiation parameters based upon the position of the sample in the core, as the flux at the sample position was insensitive to the detailed fuel structure. In the later whole core modelling of graphite and coolant gas, the fuel and the support structures holding the rods were included to better estimate the flux in the fuel channel and adjacent graphite. For the whole core models a number of calculations were made to model the core at different radial positions from the centre of the core to the radial reflector to allow the whole core to be characterised.

Reactor parameters and geometrical information pertaining to each of the models are input into the various MCNPX routines allowing the neutron behaviour to be predicted by solving the neutron transport equations. The graphite density was changed during the irradiation using estimates of graphite oxidation based upon adjacent cumulative channel irradiation. The fuel rods were replaced with fresh fuel when they achieved the average core burn-up to allow for the changes in neutron flux resulting from changes in the fuel composition during burn-up. All calculations took account of resonance self-shielding for nuclides where this is an important phenomenon, with the time steps chosen to allow this to be accurately determined during irradiation and replacement of the fuel. These neutron spectra can be calculated for any region in the model: fuel, structural materials, coolant, moderator, etc. at any height in the core or axial reflector regions and at any time during the irradiation. The voxelization was chosen to better define regions where the flux was changing rapidly; for example, the inside layers of the graphite around the fuel channels, the graphite near the ends of fuel rods and in the reflector region. The 172 neutron energy group time dependent fluxes, and where appropriate resonance self shielded grouped cross-sections, were then passed to a cross-section post processor which combined these with its own internal database of cross-sections and collapsed the cross-sections for the selected regions into three energy groups for use in FISPIN. The inventory code FISPIN determined the irradiated nuclide inventory as it changes with time, based upon reactor power, initial composition, irradiation and cooling time. In order to perform these calculations, other nuclear data are required and the standard JEF-2.2 FISPIN libraries were used.

3.2. Activation modelling results and comparison with measurement

MCNP calculations have been run for the model irradiated at the average Wylfa average power for a number of time steps until the cumulative fuel irradiation adjacent to the two measurement samples (the irradiation conditions for the two samples were near-identical). Fuel replacement being modelled during the irradiation using an average residency period for fuel rods. This was estimated from the average reactor power in the modelled region and the typical final fuel irradiation at discharge. The graphite weight loss was estimated for each cycle using a linear fall-off with adjacent cumulative channel irradiation between the reactor start-up (virgin density 1.732 g cm^{-3}) and the final value measured in the samples (~1.5 g cm^{-3}). Each burn-up cycle was modelled as a number of time-steps to allow the change of neutron flux resulting from the changes in fuel composition (U-235 burn-out, Pu-239 growth, fission product in-growth, graphite density changes, etc.).

Impurity levels for the graphite were taken from historical heat certificate data for PGA graphite (CEGB archives). In the case of the C-14 precursor N-14, a concentration of 10 wppm is listed although the method of analysis and the associated uncertainty of this value is not known. In the calculations reported here, N-14 impurity levels of zero and 10 wppm have been selected. The zero value was selected to estimate the amount of C-14 produced in the absence of the N-14 precursor. The 10 wppm value reflects what was reported in the archives but should be regarded as an arbitrary value to estimate the sensitivity of C-14 production from the nitrogen impurity. The results (activities in Bq

g^{-1}) are summarised in Table 2 together with experimentally determined C-14 values (NNL data reported indirectly in[14]).

The radiochemical analysis of the two samples had shown no evidence for surface enrichment of C-14 and, in fact, the skimmed sample (D3816) yielded a higher C-14 activity than the as-received sample (D3810). These differing measured C-14 activities are difficult to explain, particularly as D3810 shows an activity lower than that predicted from carbon precursors. Comparing the estimated and experimental results (noting this is just for two samples), the contribution of N-14 to the C-14 inventory appears low and the dominant precursor is C-13. The negative N estimation for D3810 from activation modelling makes no physical sense and simply reflects the low measured C-14 activity. It is also possible that uncertainties in the C-13 cross sections employed lead to an overestimate of C-14 from this precursor. It is unwise to attach too much significance to two measurements. While it is tempting to propose that some mechanism exists which allows an over-proportionate release of C-14 arising from C-13, this would not be consistent with the higher activity measured on D3816. The representivity of these measurements is considered further in the text below.

TABLE 2 C-14 ACTIVITY ESTIMATES (Bq g^{-1}) FOR TWO WYLFA SAMPLES BY ACTIVATION MODELLING ASSUMING DIFFERENT INPUT COMPOSITIONS COMPARED WITH THE RESULTS FROM RADIOCHEMICAL ANALYSIS

Sample	**D3816 (skimmed)†**	**D3810**
Measured (standard deviation)*	7.35E+04 (±7.2E+03)	2.72E+04 (±3.6E+03)
Predicted (10 wppm N)	9.55E+04	9.55E+04
Predicted (0 wppm N)	7.21E+04	7.21E+04
Estimated N (wppm) to match measurement	0.6	-19.2

* Standard deviation relates to measurement method uncertainty rather than C-14 variability within the material.

† Prior to measurement, this sample had 0.2 mm skimmed from its surface to investigate effects of surface contamination.

A separate study has recently been undertaken to quantify radionuclide distributions in Magnox reactor graphite [15]. This includes C-14 activities measured in graphite from the Wylfa Reactor 1 core. The results (corrected to the same mean core irradiation as the data reported here) are summarised in Figure 4 together with the data from Table 2. The samples in this study came from selected axial locations within the flattened region of the core. The data, collected from different bricks, show a large scatter compared with the reported measurement uncertainties. The measured activity for one of the samples measured for the current study (D3816) shows reasonable agreement with the data from [14], while that for the second (D3810) looks low. It is interesting to note that two samples in the peak flux region also show activities below the predicted value for zero nitrogen impurity.

Just for illustrative purposes, a flattened region axial flux shape (form factor) has been super-imposed over the measured data in Figure 4. The axial flux shape is fairly flat over much of the height of the core. Similarly the radial form factor is flat over much of the core (0.9-1.2 over ~7.5 m radius of ~8.8 m radius core). Some correlation between the measured data and the axial and radial flux shapes would be expected. The activation modelling prediction based upon 10 wppm N from the current study aligns reasonably well with the median of measurement data at mid-core height.

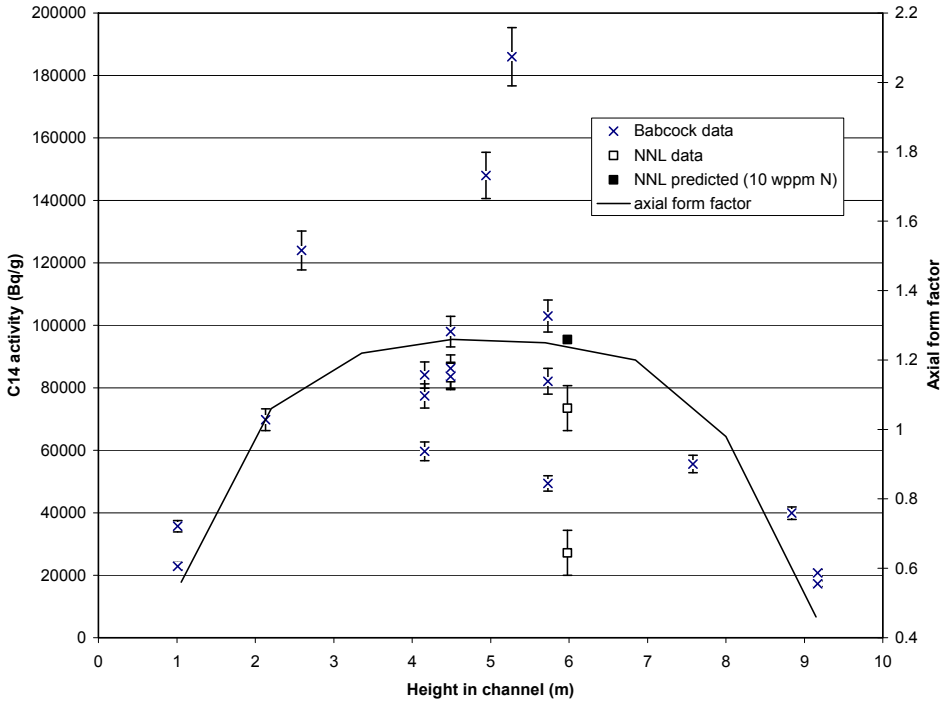

FIG. 6. Axial variation in C-14 activity in the Wylfa cores compared with activation modelling prediction

For the purposes of this study, it is assumed that a C-14 activity of 9.55×10^4 Bq g^{-1}, as calculated by the model, can be assigned to flattened region graphite in the Wylfa core at a height of 6 m above the core support plates. Furthermore, given the shape of the Wylfa radial and axial flux profiles, this activity will be typical for a large central volume of the core where the bulk of the graphite oxidation takes place. This is an informed assumption based upon prediction and measurement. In the event that a C-14 mass balance cannot be achieved using this assumption, then a more appropriate C-14 activity distribution would need to be investigated. The total amount of C-14 activity released from the whole core is evaluated below.

3.3. Mass of carbon released from core by radiolytic oxidation

The amount of C-14 activity released from the core can be estimated from the total mass of carbon released into the coolant gas circuits as carbon monoxide (CO), combined with the C-14 activity evaluated in section 3.2. The mass of carbon oxidised over the selected period can be estimated by the following methods:

- Using actual density measurements from graphite monitoring campaigns at the start and end of the selected period,

- Using weight losses from oxidation model predictions at the start and end of the selected period and

- From an analysis of CO production over the selected period.

Since each method contains different uncertainties, all three have been tested to see whether a reliable estimation can be made.

3.3.1. Method 1: density measurements

As part of the routine Wylfa core monitoring programme, samples were trepanned from the Reactor 1 core during the 2009 and 2011 outages. These samples, taken from a selection of channels in the

flattened region of the core at selected axial positions, were subsequently subjected to a range of measurements including bulk density. Each trepanned sample was sectioned into three pieces and measured to give radial information on density. The weight loss of the samples was then estimated using this measured density and an assumed virgin density. The mass of carbon released from the core through oxidation between these two outages can be evaluated from the incremental weight loss.

While the concept behind this method is simple, its implementation is not straightforward as there are complex radial and axial distributions of weight loss across the core as well as variations within bricks. The method employed was as follows:

- For the flattened region of the core, generate an axial mean brick weight loss profile based upon core monitoring data at the start and the end of the selected period. While there are weight loss distributions within brick, the mean weight loss at a given axial position can be approximated to the weight losses associated with samples originating from outer regions of the brick. Such samples are recovered by trepanning at the outside of bricks from interstitial channels.

- Fit polynomials to the interstitial channel weight losses. Using the equations for the fits, evaluate weight losses at the mid-height position of each brick layer. The mid-height weight losses are assumed to approximate to the mean brick weight loss at that layer in the flattened region of the core. The average weight loss for a column of bricks will be the mean of all the mid-height weight losses.

- The radial variation in flux across the core can be accounted for by dividing the core into concentric radial zones (zone 1 at the centre and zone 9 at the periphery) and assigning an average radial form factor to each zone. Zone 1 corresponds to the flattened region where the average weight loss of a column of bricks has been evaluated from monitoring data. Average weight losses for each of the other zones can be evaluated from the zone 1 value and the ratio of radial form factors for zone 1 and the zone under consideration.

- The volume and hence the mass of each zone can be calculated for the core at start of life. The mass loss for a given zone over the selected period can be estimated from the start-of-life mass of the zone and the incremental change in average weight loss for the zone. Evaluate the total mass loss from the sum of the zone increments.

The principal uncertainty in the method is the estimation of a representative axial weight loss profile for zone 1 from the core monitoring data. The data are summarised in Fig. 7 along with the polynomial fits. The scatter in the data is typical of within brick and between brick variability. Straight polynomial fits raise anomalies; the 2009 data seem to show higher weight losses at the top and bottom of the core than that from 2011. The average weight losses over the height of the core at 2009 and 2011 are 13.4% and 13.6% respectively. The average increment is very small and is only ~2% at the peak weight loss position. Based upon the polynomial fits, the increment will be under-estimated. The start-of-life mass of the core is calculated to be 3545 t giving a loss of carbon through oxidation between the two outages of 7.7 t.

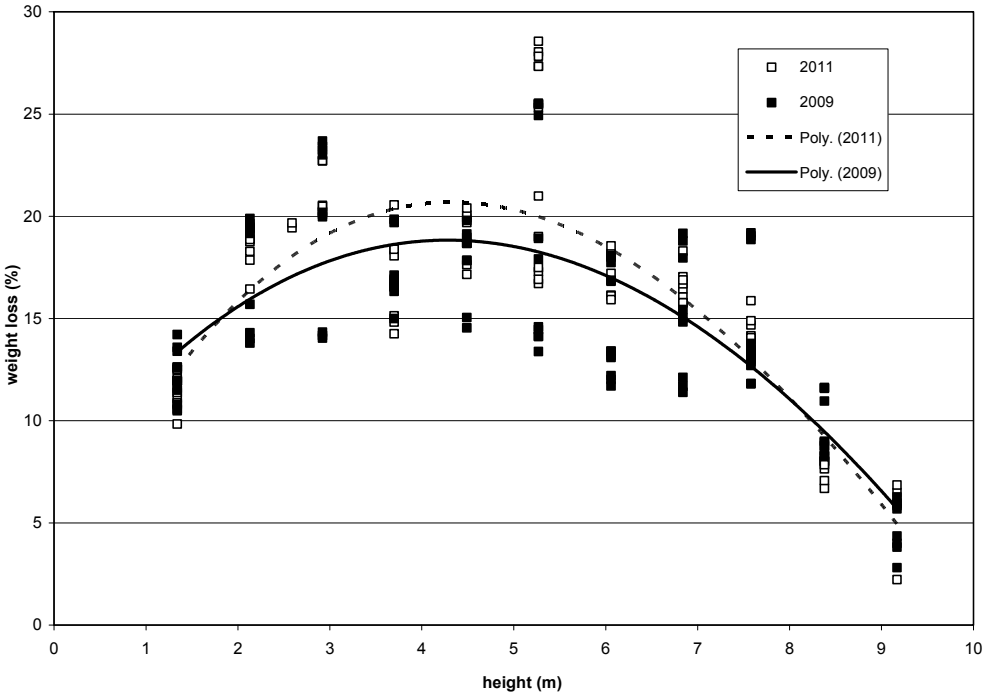

FIG.7 Interstitial channel graphite weight loss data for the Wylfa Reactor 1 core at 2009 and 2011

3.3.2. Method 2: oxidation model predictions

The semi-empirical model for radiolytic graphite oxidation BEST (not available in the open literature), which has fitting parameters that can be tuned to historical graphite monitoring data for a particular Magnox reactor, has been used to provide predictions of graphite weight losses for core structural integrity assessments. The code is available to predict weight losses at any position within a graphite core at a specified mean core irradiation. The code is also configured to evaluate the mean weight loss of an entire brick. In the case of Wylfa, the BEST code has been re-tuned periodically as new data become available and predicted mean brick weight losses for Reactor 1 have been calculated for a number of mean core irradiations. Calculated weight losses that bound the mean core irradiations for the 2009 and 2011 statutory outages are published in internal UK nuclear industry reports, from which axial flattened region mean brick weight loss profiles at these two irradiations can be evaluated. Adopting the same method as that employed in Method 1, an average weight loss for a column of bricks in the flattened region (zone 1) and for the other radial zones can be estimated. The same mass data assigned to these zones can then be used to estimate the total mass loss over the selected period.

The estimated average weight losses over the height of the core at 2009 and 2011 are 11.7% and 12.5% respectively. Based upon a start-of-life mass of the core of 3545 t and assuming shrinkage can be omitted for the purpose of this study, the loss of carbon through oxidation between the two outages will be 25.9 t. This value is significantly higher than that estimated from Method 1, with the average core weight losses being lower and the weight loss increment higher. The axial flattened region (zone 1) weight loss profiles for the two methods are illustrated in Fig. 8.

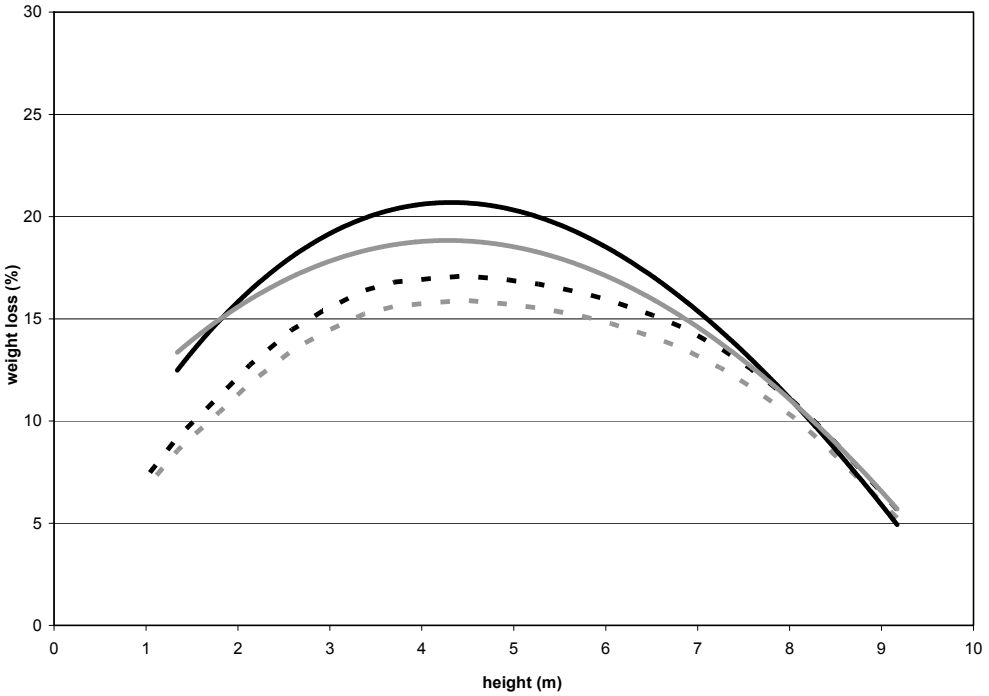

Notes : Solid curves from Method 1, broken curves from Method 2. Grey curves for 2009, black curves for 2011.

FIG.8 Zone 1 mean brick graphite weight loss profiles for the Wylfa Reactor 1 core at 2009 and 2011

For both methods, mean brick weight losses were evaluated from these curves for all graphite layers. It should be noted that the Method 1 fits are based upon methods from a single graphite monitoring campaign. Method 2 fits from BEST are based upon all historical graphite monitoring data and provide a lifetime rather than a snapshot average. The anomalous curve cross-over at the top and bottom of the core is not present when all historical data are accounted for in Method 2. As noted above, both methods rely on high accuracy in a small weight loss increment in a very large mass.

3.3.3. Method 3: carbon monoxide production

Carbon (either as graphite or carbonaceous deposit) is released as CO through its reaction with CO_2. The driver for the reaction is the amount of ionising radiation energy transferred to the CO_2 within the pores of the graphite:

$$C + CO_2 \xrightarrow{\text{ionising radiation}} 2CO$$

It is assumed that the contribution to CO production from deposits is low compared to that from the graphite. When the reactor returns to power following a statutory outage, the coolant will comprise CO_2 and residual air. . Residual air content is low as a result of CO_2 pressurisation and release cycles prior to final pressurisation and power generation. As the graphite starts to oxidise, the CO concentration in the coolant gas will gradually build up, partly offset by coolant leakage and replenishment with fresh CO_2. However, there is an upper operating limit on the CO concentration in the coolant gas and in order to control the concentration at its optimum level as a radiolytic oxidation inhibitor, a recombination unit is attached to the coolant gas circuit to remove CO by recombination with oxygen.

The station operators continuously monitor the gas coolant composition, CO_2 losses from the gas circuits (from leakage and purging) and the oxygen feed to the recombination unit. These daily records have been used to compile monthly figures and carbon release values as detailed in Table 3. Based upon these figures, the total carbon loss from the core over the period between the 2009 and 2011 outages is 16.9 t.

It is worth noting that the oxygen feed system for the recombination unit is shared between the two reactors. A check was made of CO production rates over the period when Reactor 2 was shut down for its statutory outage in 2010 and when both reactors were operating, to see whether reported oxygen feed rates to Reactor 1 were reliable. CO production rates were found to be consistent confirming the reliability of oxygen feed rates. In addition, reported CO_2 discharges were checked against calculated values based upon the decay in concentration of deliberately injected helium to the gas circuits. Reported and calculated discharges were found to be consistent.

3.3.4. Mass of carbon release – summary

The mass of carbon released from the core by radiolytic oxidation is a key input to the C-14 mass balance. For this reason, three approaches have been investigated to maximise confidence in the accuracy of the value used in the assessment.

It has been recognised that methods based upon a weight loss increment over a two-year reactor operating period will have large uncertainties as the increment is small and there will be approximations in accounting for weight loss across the whole of the core. Method 1, based upon snapshots of graphite weight loss in limited positions in the flattened region of the core at the start and end of the period of assessment, gives a total carbon mass loss of 7.7 t. Due to anomalies in the fits to the monitoring data, it is known that this value will be an underestimate. Method 2, based upon model predictions of weight loss using all historical monitoring data for the reactor, gives a total carbon loss of 25.9 t. It is not possible to say whether this value is realistic or an upper bound.

A method based upon carbon monoxide production uses CO_2 discharges and O_2 consumption data which can be measured with reasonable certainty. Furthermore, no assumptions or approximations need to be made to account for the spatial variation in oxidation across the core. This method gives a total carbon mass loss of 16.9 t, which by coincidence is mid-way between the Method 1 and 2 estimates. For the purposes of this assessment, the Method 3 carbon mass loss will be adopted, very broadly supported by the values from the other methods.

TABLE 3 WYLFA REACTOR 1 GAS COOLANT RECORDS, CO PRODUCTION AND CARBON EQUIVALENT

Period		Average thermal power (MW)	Calculated CO_2 usage per month from coolant records (t)	O_2 per month consumed in recombination unit (t)	CO_2 discharged through stack per month (t)	C removed from core per month based upon CO mass balance (kg)
Sep-09		619	193.0	0.0	189.3	568.4
Oct-09		1362	203.9	1032.0	222.1	683.2
Nov-09		1400	176.8	941.0	206.8	580.1
Dec-09		1619	206.6	1026.0	197.4	653.4
Jan-10		1470	188.1	746.0	220.6	581.7
Feb-10		1461	174.0	1002.0	197.9	595.6
Mar-10		1177	196.7	444.0	208.9	462.7
Apr-10		1476	190.3	1188.0	186.0	664.4
May-10		1245	185.5	858.0	203.3	584.2
Jun-10		1538	181.5	1531.5	186.3	824.0
Jul-10		1622	195.1	1729.0	183.8	859.1
Aug-10		1508	233.1	1411.0	205.6	806.4
Sep-10		1612	186.9	1464.0	180.4	786.6
Oct-10		1614	196.6	1617.6	205.2	853.6
Nov-10		1561	172.7	1447.9	183.6	767.2
Dec-10		1618	177.3	1487.0	189.7	812.8
Jan-11		1613	191.0	1736.0	208.3	896.3
Feb-11		1605	190.7	1445.0	174.3	767.5
Mar-11		1544	174.8	1485.0	205.0	806.8
Apr-11		1546	152.9	1378.0	184.9	755.1
May-11		1584	196.3	1500.0	182.9	771.0
Jun-11		1528	163.6	1230.0	183.7	685.7
Jul-11		1486	169.2	1254.0	180.5	714.9
Aug-11		930	128.5	588.0	120.8	379.8

3.4. Prediction of C-14 production in the coolant gas by activation modelling

The Wylfa reactor contains ~235 t of circulating CO_2, a portion of which will be irradiated giving rise to activation of the gas and its impurities. As with the graphite core, activation calculations can be made to quantify the contribution to the total C-14 inventory for the reactor from the coolant gas.

Exactly the same activation methodology as that described in section 3.1 and Ref 14 has been employed here. Further details are provided in Appendix A. As with graphite, some assumptions concerning element concentrations in the coolant must be made. For the purposes of this assessment, two gas coolant composition cases have been modelled: pure CO_2 and CO_2 with the average measured coolant N_2 concentration (44 wppm) over the selected period combined with maximum measured CO_2 feed-gas impurities (Table 4).

TABLE 4 ELEMENT CONCENTRATIONS AS INPUT TO WYLFA REACTOR 1 GAS COOLANT ACTIVATION MODELLING CALCULATIONS.

Element	**Average measured N impurity over selected period with max measured impurities in CO_2 feed-gas (mass fraction)**	**Carbon dioxide (mass fraction)**
N	2.80E-05	-
O	7.27E-01	7.27E-01
Ar	9.08E-07	-
Cl	8.06E-07	-
C	2.73E-01	2.73E-01
Ne	6.55E-11	-
He	3.75E-12	-
Kr	1.51E-11	-
H	4.58E-08	-
Xe	2.13E-12	-

The C-14 calculations take account of activation via N, O and C. Rather than taking the total mass of gas in the circuits, it is necessary to quantify gas volumes within the pores of the graphite and in the voids around the graphite in the active core (fuel channels and interstitial channels). A mass of CO_2 can then be assigned to each volume and a C-14 production rate calculated in GBq per day per tonne of coolant (in the defined volumes) per MW(thermal). Using the same graphite volume employed in Methods 1 and 2 above with void in the graphite corresponding to a 13% average weight loss and assuming that it is all accessible to the coolant, the resident irradiated mass of CO_2 is 32.6 t. With the reactor operating at 893 MW(thermal) for 700 days between the 2009 and 2011 outages, the activity of C-14 in CO_2 and in CO_2 with 44 wppm N_2 and maximum measured feed-gas impurities is 257 and 429 GBq respectively. The main uncertainties in these estimates are the accuracy of the activation calculations, the composition of the coolant and the irradiated mass of coolant in the reactor core. Of these it is expected that the accuracy of the activation calculation will lead to the largest uncertainties.

3.5. Mass balance summary

For a 6 m axial position in the flux-flattened region of the Wylfa graphite core, the C-14 activity based upon predictions assuming a 10 wppm N impurity level is 9.55×10^{4} Bq g^{-1}. It is judged that this value, which is broadly in agreement with measurements (Figure 4), will be representative of a large central volume of the core where the radial and axial flux profiles are broadly flat. Furthermore, C-14 is released from the core by radiolytic oxidation of the graphite and this oxidation process is driven by the local neutron flux. It is therefore reasonable to assume that the principal regions of the core where C-14 is produced and where radiolytic oxidation takes place are coincident and that this predicted centre-core C-14 activity can be assigned to the total mass of carbon released from the core.

An assessment of carbon release from the core as CO by radiolytic oxidation gives a mass loss of 16.9 t. This corresponds to a total C-14 release from the core to the reactor gas circuits of 1614 GBq. Activation modelling of the CO_2 coolant gas over the same period gives a total C-14 production of 429 GBq of which 172 GBq comes from nitrogen. Therefore, the total C-14 present in the gas phase, dominated by releases from the graphite, is estimated to be 2043 GBq. The C-14 will be released to the atmosphere by a combination of leakage from the gas circuits, deliberate purging and final depressurisation prior to the 2011 outage. These CO_2 releases are continuously monitored for radionuclides as described above and the total documented release from Wylfa Reactor 1 between the 2009 and 2011 outages is 1790 GBq.

4. DISCUSSION

The best estimate analysis presented here shows good agreement (within ~14%) between the predicted C-14 activity released from the graphite core and generated within the gas coolant and the measured C-14 activity discharged from the reactor over the same period. This suggests that the principle C-14 pathways have been accounted for in the abbreviated mass balance model. The analysis shows that the contribution to the total C-14 activity by activation processes in the coolant gas is relatively small (~21%). It follows that any uncertainties in the activation modelling of the coolant gas will have a low impact on the overall mass balance. Evaluating the C-14 activity release from the graphite core depends upon a credible activation modelling assessment and a reliable estimation of the mass of carbon released from the core by oxidation. In the case of the activation modelling, the assumption of a 10 wppm N impurity level in the graphite yields a C-14 activity broadly consistent with radionuclide analysis of actual core material. The estimation of the mass of carbon has been based upon CO production using reliable station records.

The implication, for a Magnox-type reactor and for Wylfa in particular, is that the C-14 precursor C-13 makes a more significant contribution (7.21×10^4 Bq g^{-1}) to the total activity than N-14 at 10 wppm (2.34×10^4 Bq g^{-1}), as shown in the calculated values in Table 4. The sensitivity of total activity of C-14 to the contributions from a fixed natural level of C-13 and varying levels of N-14 can be estimated from these values, indicating that only when the N-14 level exceeds ~30 wppm does it become the dominant C-14 precursor. The mass balance for this two year period late in reactor operational life may not reflect C-14 behaviour at other periods of operation.

As discussed in section 1.3, Doyle and Hammond [6] attempted to align measured C-14 levels in a gas-cooled reactor with predictions. While it is not possible to comment on their predictions given the absence of information on the method employed, the effluent activity measured in 1979 (eight years after reactor commissioning) would factor up to 390 MBq t^{-1} (CO_2) based upon a linear increase with time. This compares well with an average value of 370 MBq t^{-1}, for the period considered here based upon monitoring of discharges.

Bush and co-authors [7], while not underwriting their analysis with a C-14 mass balance as presented here, discuss issues associated with radionuclide predictions broadly consistent with those encountered in this study. However, they calculate that ~7% of the C-14 production (Ci GW(e)$year^{-1}$) is released to the coolant and the ratio of C-14 produced in the graphite to that produced in the coolant is ~2:1 compared with a ratio of ~4:1 in the present study.

It is instructive to review French experience with C-14 activities associated with their UNGG gas-cooled graphite moderated reactors. Poncet and Petit [16] base their assessment of radionuclide inventories on an extensive sampling and analytical study coupled with activation modelling. The activation modelling was undertaken to enable evaluation of nitrogen impurity levels consistent with the measurements. The authors report high discrepancies on radionuclide measurements, particularly for radionuclides whose precursors are present at trace levels. It is argued that poor reproducibility between analyses cannot be attributed to the quality of sampling or quality of analysis, but rather to the size of the sample combined with the heterogeneity of the graphite and the distribution of impurities in what is, paradoxically, a very pure material. They conclude that representative and reproducible analyses characterising an entire core cannot be achieved if radionuclides and impurities are present at trace levels. The uncertainties associated with radiochemical analysis are consistent with the observed scatter in the Magnox measurements reported here. The authors also observe that nitrogen impurity levels necessary to explain radiochemical measurements on French reactors are lower than those used in academic studies (such as [2]) and would need to be of the order of 4 wppm. This is broadly consistent with what has been observed here for Wylfa: model predictions with nitrogen values set to around zero align with NNL C-14 measurements; predictions with nitrogen values set to around 10 wppm align with C-14 measurements for the broader Wylfa database.

5. CONCLUSIONS

1) Records of daily C-14 discharges are maintained for all UK nuclear licensed sites. For operating nuclear plant, these are based upon C-14 activities measured in the discharge route, which can be assigned to CO_2 releases from the pressure circuits via controlled "blowdowns" (to control reactor pressure) and from normal losses from the coolant circuits during operation. The Wylfa records have provided C-14 discharge data for a selected period of operation between consecutive statutory outages on Reactor 1 between September 2009 and August 2011, which have been used for a C-14 mass balance study.

2) A C-14 mass balance model of a Magnox reactor has been devised based upon two systems: the graphite core and the coolant circuits. The model identifies all credible C-14 pathways for each of the two systems. On review, the model can be abbreviated to activation of impurities within the core graphite and their release by graphite radiolytic oxidation to the coolant and activation of the coolant itself. The total C-14 predicted by the model to be present in the gas phase can be equated with station discharge records.

3) Production rates for C-14 within the graphite have been calculated using activation modelling based upon the reactor physics code MCNPX and the fuel inventory code FISsion Product INventory (FISPIN). Predictions have been made for a position within the Wylfa Reactor 1 core where graphite has previously been retrieved and C-14 activities measured. Such predictions require a nitrogen impurity concentration input. Predictions were broadly in agreement with measurement for nitrogen impurity levels in the range 0-10 wppm.

4) Activation modelling results and measurements are broadly in agreement with historical measurements of C-14 in Wylfa core graphite. Based upon radial and axial flux distributions within the core, a global C-14 activity of 9.55×10^{4} Bq g^{-1}, appropriate to its release into the coolant by graphite radiolytic oxidation, is proposed.

5) An estimate has been made of the mass of carbon released from the graphite core by radiolytic oxidation over the selected period of analysis. Because the density change or weight loss increment averaged over the whole core is small, such an approach is highly unreliable. Instead, records of station coolant composition, gas conditioning plant history and coolant gas loss from the reactor circuits have been used to quantify the mass of carbon via the oxidation product carbon monoxide. It is estimated that 16.9 t of graphite is lost from the core between the selected consecutive outages.

6) Production rates for C-14 within the gas coolant have been calculated using the same activation model as that used for the core. In this application where coolant activation is averaged over the whole core, a general form of the model can be used for any Magnox reactor based upon station-specific coolant masses and operating histories. Predictions are based on gas volumes within the pores of the graphite and channels through the graphite in the active core rather than the total mass of gas in the circuits. Based upon a resident mass of CO_2 of 36.2 t, the C-14 activity in the coolant is calculated to be 429 GBq for gas with maximum measured impurities in the feed-gas and an average 44 wppm N_2 over the selected period.

7) The mass balance model predicts a release of 2043 GBq C-14 over the selected period. This is dominated by C-14 production from the graphite. Within the graphite, C-14 is produced from the activation of C-13 and from the activation of N-14 with an impurity level of 10 wppm. The total documented release of C-14 from Reactor 1 between the 2009 and 2011 outages is 1790 GBq.

8) The mass balance prediction is within ~14% of the reported C-14 discharge from Wylfa Reactor 1 based upon analysis for a two-year operational period. This agreement suggests that the principal C-14 pathways have been accounted for in the analysis.

9) Care should be taken in applying the findings of this analysis to other Magnox reactors and particularly to other reactor types. The mass balance for this two year period late in reactor operational

life may not reflect C-14 behaviour at other periods of operation. The analysis highlights the sensitivity of predictions to nitrogen content of the graphite. The analysis indicates that quantifying C-14 levels in graphite cores will require extensive measurement in combination with activation modelling. The C-14 measurement data for the Wylfa reactors shows considerable scatter, arising from uncertainties in radiochemical analysis, the influence of sample size, heterogeneity of the graphite and distribution of impurities.

REFERENCES

[1] NUCLEAR DECOMMISSIONING AUTHORITY, 'The 2010 UK Radioactive Waste Inventory, Report prepared for the Department of Energy & Climate Change (DECC) and the Nuclear Decommissioning Authority (NDA) by Pöyry Energy Limited'; URN 10D/985, NDA/ST/STY(11)0004 (February 2011)

[2] MARSDEN B.,J., HOPKINSON, K. L. AND WICKHAM A. J., 'The Chemical Form of Carbon-14 within Graphite'; Serco Assurance report SA/RJCB/RD03612001/R01 Issue 4, (March 2002) (www.nda.gov.uk/documents)

[3] INTERNATIONAL ATOMIC ENERGY AGENCY, 'Characterisation, Treatment and Conditioning of Radioactive Graphite from Decommissioning of Nuclear Reactors'; IAEA-TECDOC-1521, IAEA Vienna (2006)

[4] MUGHABGHAB S. F., 'Atlas of Neutron Resonances'; 5th Edition, Elsevier (2006): ISBN: 978-0-444-52035-7

[5] Environmental Permitting Regulations (England and Wales) 2010. Criteria for setting limits on the discharge of radioactive waste from nuclear sites. Environment Agency (UK) (2012)

[6] DOYLE, A. R. and HAMMOND, K., 'The Estimation of Tritium, Sulphur-35 and Carbon-14 in Reactor Coolant Gas and Gaseous Effluents, Symposium on Management of Gaseous Wastes from Nuclear Facilities'; IAEA-SM-245/33, IAEA Vienna (1980)

[7] BUS, R. P., WHITE I. F., and SMITH G. M., 'C-14 Waste Management'; CEC, Euratom Report EUR-8749 (1984)

[8] WICKHAM A.J., 'Caring for the Graphite Cores'; IMechE Seminar The Review of Safety at Magnox Nuclear Installations, IMechE London (1989)

[9] YIM M-S., and CARON F., 'Life cycle and Management of Carbon-14 from Nuclear Power Generation, *Progress in Nuclear Energy* Issue 1, **48**, *pp.* 2-36 (2006)

[10] ASTM D6556 – 10, Standard Test Method for Carbon Black-Total and External Surface Area by Nitrogen Adsorption

[11] DUNZIK-GOUGAR M. L., 'Characterisation and Treatment of 14-C on Irradiated Graphite Surfaces'; *13th International Nuclear Graphite Specialists Meeting*, Meitingen, Germany (September 2012)

[12] PELOWITZ D. B., MCNPX Users Manual, Version 2.6.0 (2008)

[13] FISPIN for Nuclide Inventory Calculations: Introductory Guide for Version 10, Report

ANSWERS/FISPIN/REPORT/001 published by Serco Assurance Ltd (2007)

[14] MILLS R. W., RIAZ Z., and BANFORD A. W., 'Nuclear Data Issues in the Calculation of C-14 and Cl-36 in Irradiated Graphite'; ENC2012, European Nuclear Conference Manchester, UK (December 2012)

[15] LANSDELL T., and NEWLAND M., 'Magnox Reactor Graphite Characterisation Stage 2 – Final Active Analysis Stage'; Babcock Report TSG(11)0801 (October 2012) (www.nda.gov.uk/documents).

[16] PONCET B., and PETIT L., 'Method to Assess the Radionuclide Inventory of Irradiated Graphite Waste from Gas-Cooled Reactors'; J. Radioanalytical and Nuclear Chemistry, **298**, *pp.* 941-953 (2013): DOI 10.1007/s10967-013-2519-6

APPENDIX A - CALCULATION OF CARBON DIOXIDE ACTIVATION

The calculation of activation within the coolant requires the amount of C-14 precursors (C, N and O isotopes) in the different parts of the core and the neutron flux, and their spectra within these volumes. If we assume that the stable C-14 precursors in the coolant are only negligibly depleted during reactor operation and that decay of C-14 has a long half-life compared to the irradiation time, then the production of C-14 can be calculated in each region using:

$$\delta N_{C14} = \phi \left(N_{C13}\, \sigma_{C13->C14} + N_{N14}\, \sigma_{N14->C14} + N_{O17}\, \sigma_{O17->C14}\right)$$

In this work, we consider a whole Magnox core split into 52 axial slices modelled in the central flattened power region and at 4 radial positions around this. The radial regions are interpolated and extrapolated into 37 radial regions. This gives 1924 modelled regions, each of which is split into a series of sub-regions including fuel, cladding, coolant and the graphite. The graphite is further split into a series of concentric regions around the fuel channels.

It should be noted that Magnox reactors vary considerably in size and power, but due to commonalities in the neutronic design and the neutron cross-sections of graphite they have a highly thermal neutron spectrum whose flux is proportional to the local reactor power. The major differences in activation modelling arise from the reactor power and the graphite oxidation within the core.

MCNP can only tally the flux during interactions, thus in the above modelling, it was impractical to estimate the flux in the coolant within the fuel and interstitial channels. However, these fluxes will be almost identical to the flux seen in the first graphite region around the fuel and the graphite region around the interstitial and control rod channels respectively. Also, as neutrons have a range in graphite considerably larger than the size of the pores, it can be assumed that the coolant in the pores will see the same flux as the bulk graphite interactions.

Coolant activation

To allow comparisons to be made between different reactors, the modelled fluxes were chosen at the end of life of the modelled Oldbury reactor and these were used to irradiate 1 tonne of coolant. As will be discussed below, coolant activation averaged over a whole core will be broadly insensitive to neutron spectra effects and power shape. Calculations of coolant activation based upon the Oldbury model will be applicable to any Magnox reactor provided the mass of coolant and power history are available. The reactor averaged C-14 production rate per MW (thermal) per tonne of coolant in all the graphite regions (coolant in pores), surface layer of graphite in fuel channels (fuel channel coolant) and bulk graphite region furthest from the fuel surrounding the interstitial and control channels (interstitial and control rod channel coolant) were then calculated. The compositions considered are given in Table A1 and the C-14 production rates (GBq per MW per tonne of coolant) in Table A2. It is noted that irradiation of air (i.e. 78% nitrogen instead of ppm in carbon dioxide) results in a 10,000-fold increase in the C-14 production rate, so care must be taken in understanding the nitrogen/air that may be introduced to the core during blowdowns. Following a depressurization, and subsequent purges, it was found that the nitrogen content is the coolant gases is raised above those measured in the coolant feed, but below the maximum permitted. However, this reduces with time as more coolant is fed to the core to replace losses. The mean measure nitrogen content of the core was found to 44 volume ppm of nitrogen gas during the period being modelled.

A sensitivity study showed that the effect of using the start of life graphite density resulted in a C-14 inventory differing by less than 1% from the end of life values for coolant consisting of carbon dioxide or carbon dioxide with maximum measured impurity levels. Higher nitrogen content increased this difference slightly, but the change is still within a few percent, showing the effect on the coolant activation of graphite oxidation is small.

TABLE A1 COOLANT COMPOSITIONS CONSIDERED IN STUDY – MASS FRACTIONS

Element	Dry air	Max allowed coolant impurities	Max measured coolant impurities with 44 vppm nitrogen	Max measured coolant impurities	Carbon dioxide
Volume N_2 %	78.09	8.0E-3	4.4E-3	6.2E-4	0
N	7.55E-01	5.09E-05	2.80E-05	3.95E-06	-
O	2.32E-01	7.27E-01	7.27E-01	7.27E-01	7.27E-01
Ar	1.28E-02	9.08E-07	9.08E-07	9.08E-07	-
Cl	0.00E-00	8.06E-07	8.06E-07	8.06E-07	-
C	1.25E-04	2.73E-01	2.73E-01	2.73E-01	2.73E-01
Ne	1.25E-05	8.45E-10	6.55E-11	6.55E-11	-
He	7.19E-07	4.84E-11	3.75E-12	3.75E-12	-
Kr	2.89E-06	1.95E-10	1.51E-11	1.51E-11	-
H	3.13E-07	2.29E-07	4.58E-08	4.58E-08	-
Xe	4.08E-07	2.75E-11	2.13E-12	2.13E-12	-

TABLE A2 C-14 PRODUCTION RATE IN DIFFERENT REGIONS FOR A RANGE OF COOLANT COMPOSITIONS

Core averaged C-14 production rate in GBq per day per tonne of gas per MW during a day's irradiation	Dry Air	Max allowed coolant impurities	Max measured coolant impurities with 44 vppm nitrogen	Max measured coolant impurities	Carbon dioxide
Fuel channel coolant	2.22E-01	2.75E-05	2.08E-05	1.37E-05	1.25E-05
Graphite pore coolant	2.29E-01	2.81E-05	2.11E-05	1.38E-05	1.26E-05
Interstitial/CR channel coolant	2.35E-01	2.87E-05	2.16E-05	1.41E-05	1.29E-05

TABLE A3 C-14 PRODUCTION RATE SENSITIVITY TO GRAPHITE DENSITY

Material irradiated	Region	Core averaged C-14 production rate GBq per day per tonne of gas per MW (thermal)		Ratio of final/initial rate
		Start of life (0 days)	End of Life (12465 days)	
CO_2	Fuel channel	1.24E-05	1.25E-05	0.99
	Bulk graphite	1.26E-05	1.26E-05	0.99
	Interstitial/CR	1.29E-05	1.29E-05	1.00
CO_2 max measured coolant impurities	Fuel channel	1.36E-05	1.37E-05	0.99
	Bulk graphite	1.39E-05	1.38E-05	1.00
	Interstitial/CR	1.42E-05	1.41E-05	1.01
CO_2 max measured coolant impurities with 44 vppm nitrogen	Fuel channel	2.08E-05	2.08E-05	1.00
	Bulk graphite	2.13E-05	2.11E-05	1.01
	Interstitial/CR	2.20E-05	2.16E-05	1.02
CO_2 max allowed impurities in specification	Fuel channel	2.77E-05	2.75E-05	1.01
	Bulk graphite	2.85E-05	2.81E-05	1.01
	Interstitial/CR	2.94E-05	2.87E-05	1.02
Air	Fuel channel	2.27E-01	2.22E-01	1.02
	Bulk graphite	2.36E-01	2.29E-01	1.03
	Interstitial/CR	2.45E-01	2.35E-01	1.04
Graphite density starts at 1.732 g cm^{-3} and at 12465 days has a minimum density of 1.112 g cm^{-3} in the central region (~36% wt loss)				

As the graphite weight loss has little effect on the coolant activation when averaged over the whole core (unless significant nitrogen is present), it is expected that the neutron spectra effects within the core are small and thus the power shape within the core will not strongly alter the results. It is thus expected that the above figures can be used for any Magnox reactor provided the mass of coolant and power history are available.

Graphite pore volume

The Wylfa core has a graphite volume of 2498 m^3. Initially the pore volume fraction is 0.20 but this increases to 0.33 at the time of the modelling. Thus the pore volume is 824.34 m^3 and it is assumed that it is all accessible to the coolant gas.

Fuel channel coolant volume

There are 6156 fuel channels in each Wylfa core (noting the presence of 6 plugged channels on Reactor 1 will have a negligible impact on the calculations). The fuel channels are 98.1 mm in diameter and each contains 8 fuel elements. The fuel channels extend over the entire 10.3 m height of the core. The volume of a single empty fuel channel is 0.08 m^3 and the total volume of all the empty channels is 479.20 m^3.

However, this includes the volume of the fuel elements comprising a uranium bar clad in Magnox alloy. Based upon a fuel design cladding volume of 990 cm^3, an inner cladding diameter of 28.26 mm and a fuel element length of 1118.61 mm, the volume occupied by eight fuel assemblies in a channel is 0.0135 m^3.

A single fuel channel gas volume is therefore 0.0643 m^3 and the total gas volume for 6156 channels is 395.90 m^3.

Control rod and interstitial channels

The Wylfa reactors each contain 380 control rod channels with an inner diameter of 108mm and 384 channels of an inner diameter of 95.3 mm for flux flattening, instrumentation etc. For the purposes of these calculations, it is assumed that all 764 channels are empty and have a gas volume of 64.07 m^3.

Volumes of all regions and predicted activation

The 6156 fuel channels (minus the fuel elements) contain 395.90 m^3 of coolant and the interstitial and control rod channels 64.07 m^3. The volume of control rods and other items in the interstitial channel are unknown and are ignored in this calculation. The Wyfla reactor has an input temperature of 234°C and output of 370°C and a pressure of 27.6 kg cm^{-2}. This gives an average density of the coolant of 25.39 kg m^{-3}. Table A4 summarises C-14 production in the coolant based on the Wylfa reactor operating at 893 MW(thermal) for 700 days between the 2009 and 2011 outages.

The nitrogen content of coolant following a blowdown with air was measured as 44 volume ppm and thus the values from these figures were used to estimate the coolant activation. Any air trapped in the graphite pores would further increase the activation, but unless this leaked into the coolant it would have not effect on discharges.

TABLE A4 C-14 PRODUCTION IN THE COOLANT DURING THE 700 DAYS OF OPERATION BETWEEN 2009 AND 2011

Region	Volume of coolant (m^3)	Mass of coolant (t)	C-14 (GBq) in CO_2 with maximum measured impurities and 44 volume ppm nitrogen	C-14 (GBq) in CO_2
Coolant in fuel channels	395.90	10.05	130.57	78.81
Coolant in graphite pores	824.34	20.93	276.39	165.14
Coolant in CR/interstitial channels	64.07	1.63	21.95	13.08
Total	1284.31	32.61	428.91	257.03